Preferential Oxidation of Zinc Finger 2 in Estrogen Receptor DNA-binding Domain Prevents Dimerization and, Hence, DNA Binding†

Randy M. Whittal,‡ Christopher C. Benz,§ Gary Scott,§ Jenia Semyonov,§ Alma L. Burlingame,‡,|| and Michael A. Baldwin*,‡,⊥

Mass Spectrometry Facility, Department of Pharmaceutical Chemistry; Oncology-Hematology/Cancer Research Institute; the Liver Center; Department of Neurology and Institute for Neurodegenerative Diseases; University of California, San Francisco, California 94143

Received February 7, 2000; Revised Manuscript Received May 3, 2000

ABSTRACT: For approximately one-third of estrogen receptor (ER)-positive breast cancer patients, extracted tumor ER is unable to bind to its cognate DNA estrogen response element (ERE), an effect that is partly reversible by the thiol-reducing agent dithiothreitol (DTT). Full-length (67 kDa) ER or its 11 kDa recombinant DNA-binding domain (ER-DBD) is also susceptible to loss of structure and function by the action of oxidants such as diamide and hydrogen peroxide; however, prior DNA binding by ER or ER-DBD protects against this oxidant induced loss of function. The ER-DBD contains two $(Cys)_4$-liganded zinc finger motifs that cooperate to stabilize a rigid DNA-binding recognition helix and a flexible helix-supported dimerization loop, respectively. Comparisons between synthetic peptide analogues of each zinc finger and recombinant ER-DBD in the presence of zinc by electrophoretic mobility shift assay, circular dichroism, and mass spectrometry confirm that cooperativity between these zinc fingers is required for both ER-DBD structure (α-helicity) and function (dimeric DNA binding). Rapid proteolytic digestion of monomeric, non-DNA-bound ER-DBD followed by HPLC-MS analysis of the resulting peptides demonstrates that zinc inhibits thiol oxidation of the DNA-binding finger, but not the finger supporting the flexible dimerization loop, which remains sensitive to internal disulfide formation. These findings indicate that the loss of ER DNA-binding function in extracts from some primary breast tumors and in ER or ER-DBD exposed to thiol-reacting oxidants results from this asymmetric zinc finger susceptibility to disulfide formation that prevents dimerization. Although ER-DBD contains several strategically located methionine residues, they are less susceptible to oxidation than the thiol groups and, thus, afford no protection against cysteine oxidation and consequent loss of ER DNA-binding function.

The DNA-binding and transactivating functions of many transcription factors are redox sensitive, and most of these factors appear to be regulated via oxidation of critical cysteine residues within their DNA-binding domains (DBDs).[1] In particular, transcription factors such as Sp1 and the steroid-binding glucocorticoid receptor (GR) contain redox-sensitive cysteine residues supporting the zinc-finger structures necessary for binding to the major groove of DNA. Although there is no significant age-related decline in the tissue content of Sp1 or GR, aging causes in vivo accumulation of oxyradical tissue damage and consequent selective loss of the DNA-binding activities of these proteins (*1*, *2*).

The estrogen receptor (ER) containing two $(Cys)_4$-liganded zinc fingers homologous to GR is similarly redox sensitive, consistent with the observation that its transcriptional activity and DNA-binding capacity are modulated by the redox effector protein, thioredoxin (*3*). Many zinc fingers employ histidine in place of one or more cysteine residues (*4*); indeed, each of the Sp family members contains three highly homologous Cys_2His_2 zinc fingers (*5*). Metallothionein can donate zinc ions to ER, or it can abstract zinc in situations of zinc deprivation (*6*). Biophysical studies on recombinant

† This work was supported by NIH CA71468. The UCSF Mass Spectrometry Facility was supported by NIH NCRR RR01614. The UCSF Computer Graphics Laboratory was supported by NIH P41 RR01081.

* To whom correspondence should be addressed at Box 0446, UCSF, CA 94143-0446 Phone: (415) 476 3813. Fax: (415) 502 1655. E-mail: mikeab@itsa.ucsf.edu.

‡ Mass Spectrometry Facility.

§ Oncology-Hematology/Cancer Research Institute.

|| Liver Center.

⊥ Department of Neurology and Institute for Neurodegenerative Diseases.

[1] Abbreviations: ER, estrogen receptor; DBD, DNA-binding domain; ER-DBD, recombinant His-tagged estrogen receptor DNA-binding domain, ERE, estrogen response element; GR, glucocorticoid receptor; VDR, vitamin D receptor; LBD, ligand binding domain; EMSA, electrophoretic mobility shift assay; HPLC, high-performance liquid chromatography; IMAC, immobilized metal ion affinity chromatography; MS, mass spectrometry; ESI-MS, electrospray ionization mass spectrometry; oa-ToFMS, orthogonal acceleration time-of-flight mass spectrometer; TIC, total ion current; CD, circular dichroism spectroscopy; NMR, nuclear magnetic resonance spectroscopy; DTT, dithiothreitol; IPTG, isopropyl-*β*-D-thiogalactopyranoside; TFA, trifluoroacetic acid; IAA, iodoacetic acid; ZF, zinc finger; Pep1, peptide corresponding to $Lys_{16}-Gln_{50}$ of ER-DBD; Pep2, peptide corresponding to $His_{52}-Lys_{88}$ of ER-DBD; poly[d(I−C)], polydeoxyinosinic-deoxycytidylic acid.

10.1021/bi000282f CCC: $19.00
Published on Web 06/27/2000

ER-DBD demonstrated reversible loss of DNA binding and α-helical structure upon oxidation but irreversible loss of these properties following cysteine alkylation (*7*). A significant proportion of breast cancer patients fail to respond to treatment with the antiestrogen, tamoxifen, possibly due to structural defects in their ER. We previously established that tumors from these patients often express ER that is incapable of forming ER-ERE complexes in vitro (*8*−*10*). It seems likely that oxidation is the basis for this functional defect since the DNA binding by ER contained in these primary tumor extracts can often be restored by vigorous thiol reduction, and this same functional abnormality can be induced in ER-expressing breast cancer cells briefly exposed to oxidants in vitro (*7*).

Here we have employed mass spectrometry (MS) to study the structural consequences of recombinant ER-DBD oxidation. There have been several previous MS studies of nuclear hormone receptors, including ER. Two cysteines in rat ER-ligand-binding domain (LBD), particularly Cys-447, were shown to be protected from alkylation by ligand binding (*11*). Selective proteolysis and MS analysis of the peptide products of this 33 kDa ER-LBD complexed with estradiol identified a protease resistant core, amino acids 304−509, which was sufficient for ligand binding, although flexibility and accessibility to cleavage at 465−468 suggested the existence of two subdomains. The C-terminal extension 530−553, known to contain elements essential for the ligand-binding modulation of transcription activation, proved to be highly solvent-accessible (*12*). Electrospray ionization mass spectrometry (ESI-MS) (*13*) is highly effective for monitoring noncovalent associations (*14*, *15*). ESI-MS was used to show that ER-LBD can exist as a dimer having either zero or two molecules of bound estradiol (*16*). Several MS studies of the DBD domains of ER and other nuclear hormone receptors have concentrated on their metal-binding properties, as these DBDs possess $(Cys)_4$-liganded zinc fingers that are essential for normal activity. Consistent and contemporaneous with an electrophoretic mobility shift assay (EMSA) study (*17*), an ESI-MS study showed that copper can replace zinc in ER-DBD, possibly with higher affinity and with the higher stoichiometry of two copper ions per zinc finger (*18*, *19*). A similar ESI-MS study of metal binding by GR-DBD showed binding of two cadmium ions as an alternative to zinc (*20*). Complexes of the vitamin D receptor (VDR)-DBD, metal ions, and the appropriate double-stranded DNA response element were also studied by ESI-MS; either zinc or cadmium divalent cations (M^{2+}) allowed the formation of VDR-DBD_2·$M^{2+}{}_4$·DNA, although surprisingly, the presence of excess metal ion caused dissociation of these complexes (*21*).

Structural studies by NMR and X-ray crystallography have established that the functional form of ER-DBD that binds to DNA is dimeric, with its two zinc fingers serving two different functions, the first acting as the major groove DNA-binding motif and the second responsible for dimer stabilization (*22*−*24*). The NMR solution structure shows that the second finger in the dimerization motif is more flexible and less well structured, consequently, it might be anticipated that this finger can be disrupted more easily by such a process as oxidation. If so, oxidation of this finger would have the major effect of preventing or destabilizing both ER-DBD dimerization and DNA binding.

MATERIALS AND METHODS

Test reagents (diamide, iodosobenzoate, menadione, iodoacetamide, H_2O_2, and DTT) were all obtained commercially (Sigma, St. Louis, MO). Zinc(II) sulfate was purchased as 0.5 M solution (Aldrich, Milwaukee, WI). The buffer for the zinc-binding studies was ammonium acetate (Fluka, Milwaukee WI), adjusted to pH 7.4 with ammonium hydroxide (Mallinckrodt, Paris, KY). The pH was recorded after the addition of metal ions and peptides.

Expression and Purification of Recombinant ER-DBD. A T7 expression system was used for recombinant bacterial expression of human ER-DBD (*25*). The entire DBD domain of human ER (amino acids 179−262) was PCR amplified from full-length ER cDNA using the primers ER-DBDu (5′-CTAGCTAGCGCCAAGGAGACTCGCTACTG-3′) and ER-DBDw (5′-CGTAAGCTTCACCCTCCTCTTCGGTCT-TTTCG-3′), as previously described (*26*). After restriction enzyme digestion with *Nhe*I and *Hin*dIII (underlined sites), the DNA fragment was cloned into *Nhe*I−*Hin*dIII digested pRSETA (Invitrogen), yielding plasmid pRSETA-hER-(DBD). This plasmid enables expression of ER-DBD under the control of the phage T7 promoter with a peptide tag (MetArgGlySer$[His]_6$) fused to the N-terminus for protein purification. IPTG-induced cultures of transformed *Escherichia coli* were harvested and resuspended in a cold nickel-column binding buffer (Novagen), sonicated, and the urea-solubilized material collected by centrifugation. ER-DBD was purified by nickel immobilized ion affinity chromatography (IMAC) under denaturing conditions, then renatured by dialysis to remove urea, checked for protein size and integrity by Western blotting, and the eluate stored at −80 °C. Aliquots for EMSA analysis were employed directly. Samples for structural studies were either dialyzed against 0.1 mM DTT or purified by HPLC.

Synthetic Peptides. Two amino acid sequences were selected from ER-DBD for synthesis as peptides to contain the two zinc fingers and their associated C-terminal helical regions, respectively (Figure 1). These were synthesized commercially (Alpha Diagnostic, San Antonio, TX) as C-terminal amides, designated Pep1 and Pep2 (Figure 1). They were further purified by reversed-phase HPLC and their molecular masses were confirmed by ESI-MS: Pep1 calculated, 4067.84 Da; measured, 4067.99 Da; Pep2 calculated, 4394.03 Da; measured, 4392.90 Da, based on monoisotopic masses.

EMSA. ER-DBD was assayed for DNA-binding (ER-ERE complex formation) as previously described (*7*−*10*, *26*). ESX-DBD was used as a control. Briefly, buffer or reagent-treated extracts were incubated with 1−2 mg/mL poly[d(I−C)] in 100 mM KCl, 10 mM Tris·HCl, pH 7.5, 2 mM DTT, and 20% vol/vol glycerol for 20 min at 4 °C. In some experiments, selected protein samples were treated with 10 mM EDTA. The binding reaction was then initiated by adding 10 fmol (4×10^4 cpm) of ^{32}P-5′ end-labeled ERE-containing DNA probe to the reaction mix, which was incubated for another 20−30 min at 20 °C. Some protein samples were treated with 0.1, 0.5 or 1 mM diamide, either before or after binding to DNA. DNA-bound (ER-ERE) complexes and free probe were electrophoretically separated on 4.2% acrylamide (29:1 acrylamide:bisacrylamide) gels in

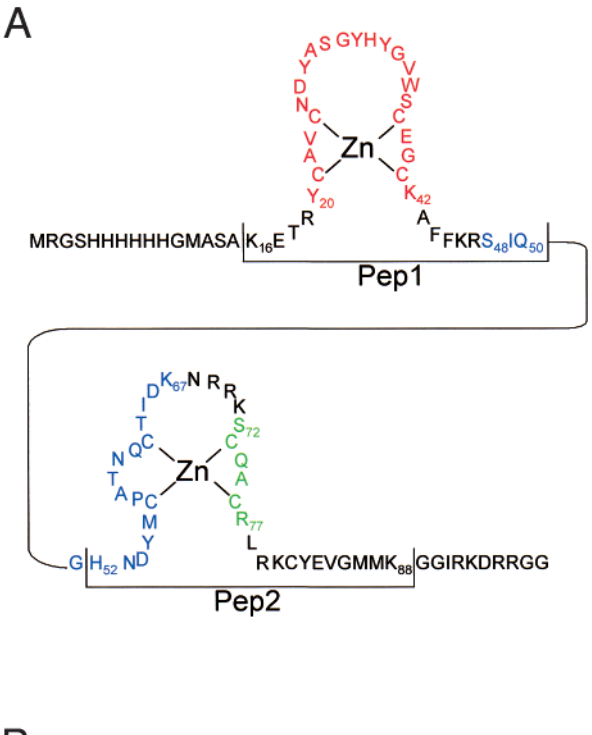

FIGURE 1: (A) Amino acid sequence of recombinant ER-DBD expressed and used in this study. Horizontal brackets show the sequences for the synthetic peptides Pep1 (Lys_{16}−Gln_{50}) and Pep2 (His_{52}−Lys_{88}). Tryptic peptides Tyr_{20}-Lys_{42} (red), Ser_{48}-Lys_{67} (blue), and Ser_{72}−Arg_{77} (green) are representative of those used to monitor differential oxidation of the two zinc fingers. (B) Multiple structures from NMR analysis of ER-DBD monomer free in solution, showing the more flexible and exposed nature of finger 2 associated with the dimerization domain compared with finger 1 of the DNA recognition domain (coordinates from ref *24*). The zinc finger cysteine residues are shown in yellow and the zinc ions in silver.

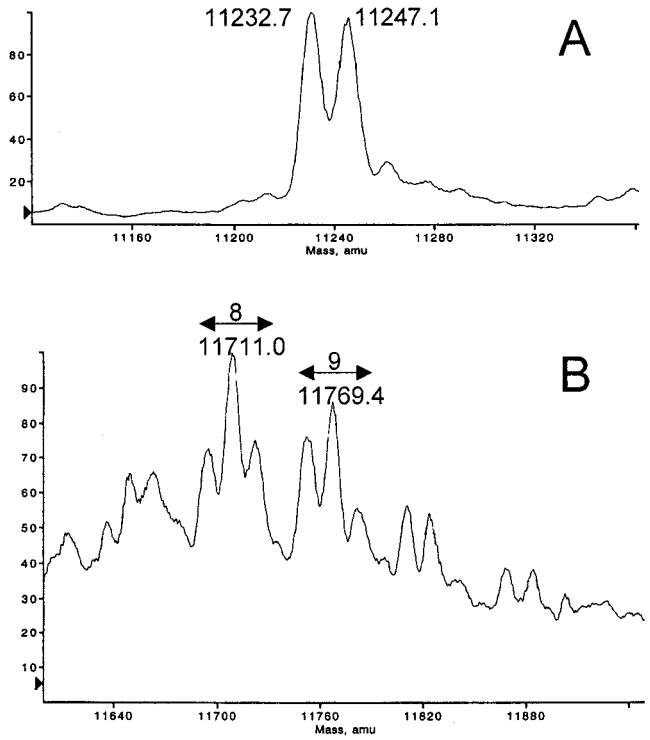

FIGURE 2: (A) Deconvolution of HPLC-MS data for ER-DBD: measured M_r, 11232.7 Da; calculated, 11232.9 Da. The coeluting component of higher mass was found to be methylated at the N-terminus: measured M_r, 11247.1 Da; calculated, 11246.9 Da. (B) The same sample treated with iodoacetic acid to carboxymethylate the nine free cysteine residues, with the expected addition of 58 mass units per alkylation. There was a distribution of alkyl groups added, maximizing at 8 and 9. Three peaks were observed for each alkylation, as indicated (↔); the labeled peaks are the methylated species, usually the most abundant.

0.5× TBE (50 mM Tris, pH 7.5, 50 mM boric acid, and 1 mM EDTA) running buffer at 150 V. Gels were vacuum-dried and visualized by autoradiography. The DNA probe used in these and earlier studies (*7*−*10*, *26*) was composed of duplexed oligodeoxynucleotides (35-mers) with the ERE-containing sense strand sequence 5′-GTCCAAAGTCAG-GTCACAGTGACCTGATCAAAGTT-3′.

ESI-MS and HPLC-MS. ESI-MS was carried out using two different mass spectrometers. Initial studies on the purity of ER-DBD and the oxidation and reduction studies (Figures 2 and 3) were monitored using the first quadrupole of a triple quadrupole mass spectrometer (PE Sciex API 300, Concord, Ontario, Canada) equipped with an electrospray ionization (ESI) source. Samples were desalted by HPLC-MS, using an Applied Biosystems 140B HPLC (PE Biosystems, Foster City, CA) fitted with a Vydac 150 × 1.0 mm C-18 microbore column with 300 Å pore size and 5 μm particle size. Solvent A was water with 0.06% trifluoroacetic acid (TFA) to control pH, and solvent B was 80% acetonitrile/0.052% TFA at a flow rate of 50 μL/min. Initial conditions of 10% B were maintained for 10 min, followed by a linear gradient to 60% B over 60 min. The column effluent passed through a 35 nL UV flow cell, then was split such that ∼10% passed into the ESI source of the mass spectrometer and the balance was collected in fractions for later studies. Accumulated mass spectra were recorded continuously throughout the running of each sample at intervals of 5 s. The UV-chromatogram recorded at 210 nm was compared with the total ion current (TIC) trace obtained from the mass spectrometer. ESI spectra corresponding to peaks in the UV and TIC traces were selected manually for averaging and deconvolution using the software provided by the mass spectrometer manufacturer.

Mass spectrometer 2, which was used for all other studies, was an orthogonal acceleration time-of-flight mass spectrometer (oa-ToFMS) (Mariner, PE Biosystems, Framingham, MA) equipped with an ESI source and an ion mirror (reflectron). A syringe pump (Harvard Apparatus, Holliston, MA) provided a stable liquid flow at 1−3 μL min^{-1} to the ESI source. The analysis of zinc binding to reduced ER-

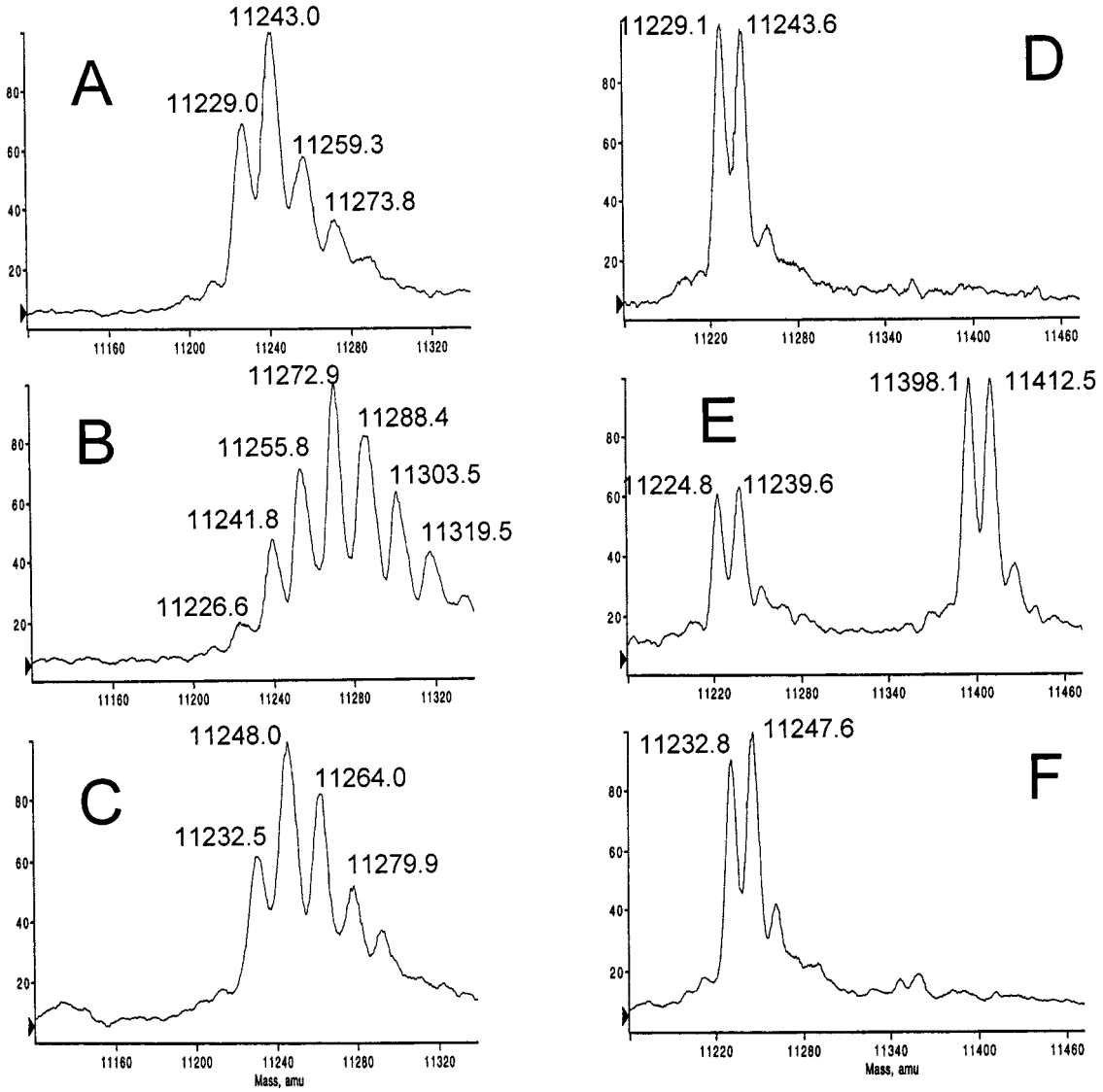

FIGURE 3: Deconvolution of HPLC-MS data obtained from oxidation of ER-DBD by H_2O_2 or diamide. (A) After oxidation with 5 mM H_2O_2 for 25 min (loss of four Hs). (B) After oxidation with 5 mM H_2O_2 overnight (loss of six Hs). (C) After oxidation with 5 mM H_2O_2 for 25 min then reduction with 50 mm DTT (fully reduced). (D) After oxidation with 5 mM diamide for 30 min (loss of four Hs). (E) After oxidation with 25 mM diamide for 30 min (loss of eight Hs plus addition of diamide). (F) After oxidation with 25 mM diamide for 30 min then reduction with 125 mM DTT (fully reduced).

DBD was carried out by infusing 5−10 μM ER-DBD in 2.5 mM ammonium acetate solution, pH 7.4, in the presence of 100 μM dithiothreitol (DTT) with 10% methanol added. The Zn^{2+} concentration was adjusted by dilution of a 0.05 M zinc(II) sulfate stock solution. Each solution was infused for approximately 20 min, and then the spectra were recorded and averaged over 5 min. Studies on the purity and oxidation state of the ER-DBD protein and the zinc finger peptides were carried out by infusing a 10 μM solution of the protein or peptide in 1:1 H_2O/MeOH with 0.1% acetic acid added. In addition, the purity and oxidation state were assessed by HPLC-MS using the HPLC described above interfaced to mass spectrometer 2. Approximately 100 pmol of ER-DBD protein or 200 pmol of zinc finger peptide was injected onto a Vydac 150 × 1 mm C-18 microbore column. Solvent A was 0.1% TFA and solvent B was 0.08% TFA in acetonitrile, at a flow rate of 50 μL min^{-1}, with a linear gradient of 10 to 60% solvent B over 60 min.

For intact ER-DBD, the isotopic components at adjacent masses could not be resolved by either mass spectrometer; therefore, the measured mass of each peak represented an average of the distribution of all isotopes present. These were compared with values calculated from average atomic masses. For Pep1 and Pep2 and for peptides from tryptic digestion, the isotopic clusters were resolved by mass spectrometer 2 to give separate peaks, and the masses were measured for the first peak within each isotopic cluster, corresponding to the monoisotopic molecular mass. Each molecular species gave one or more peak clusters arising from different charge states. In general, quantitative data were derived from the mass spectra by addition of the signal intensities from all of the individual charge states. Alternatively, deconvolution was employed to convert each series of multiply charged ions of different *m*/*z* values into a zero charge spectrum, using software provided with the mass spectrometers. This format showed molecular mass directly, as in Figure 2.

Alkylation of ER-DBD. ER-DBD that had been reduced with 2 mM DTT was incubated with 6 mM iodoacetic acid at 4 °C for 1 h, causing the addition of carboxymethyl groups

to free cysteines. The product was purified and analyzed by HPLC-ESI-MS.

Oxidation of ER-DBD. Initial oxidation experiments were carried out with either 5 mM hydrogen peroxide or 5 or 25 mM diamide for periods extending from 25 min to overnight. The extent and nature of the oxidation were evaluated by HPLC-MS of the intact protein. Subsequent titrations with oxidizing agents were carried by incubating 10 μM reduced ER-DBD (previously stored in 100 μM DTT) in 11.5 mM ammonium acetate, pH 7.4, and either 60 μM zinc(II) sulfate or 100 μM Na_2EDTA with various concentrations of either hydrogen peroxide or diamide. The oxidation was allowed to proceed for 15 min before analysis by rapid tryptic digestion. For rapid enzymatic digestion of ER-DBD protein, the protein was injected onto a Porozyme-packed immobilized trypsin column (PE Biosystems, Framingham, MA) at a flow rate of 50 μL min^{-1}. The digestion buffer was 70 mM ammonium bicarbonate/5% acetonitrile, pH 8.0, from which dissolved air had been removed by vacuum filtration followed by helium purging and continuous helium bath at 3 psi. The pH was checked and adjusted with acetic acid or ammonium hydroxide before each analysis. The enzyme column was connected in series via a Rheodyne switching valve to a Vydac 150 $\times$ 1 mm C-18 microbore column. After 3 min, the valve was switched to allow analysis of the resulting peptides by HPLC-MS at a flow rate of 50 μL min^{-1}. The enzyme column was rinsed after each analysis with at least 10 mL of digest buffer. For the HPLC analysis, solvent A was 0.1% formic acid and solvent B was 5:2 ethanol/*n*-propanol with 0.05% formic acid; both solvents were vacuum filtered and purged with helium then continuous helium bath at 3 psi. After holding at 5% solvent B for 2 min, a linear gradient was run from 5 to 60% solvent B in 30 min. The eluted peptides were passed through a micro UV flow cell with detection at 210 nm and the flow was split to transfer ~10% to the ESI source. Oxidation by hydrogen peroxide was also monitored by CD (see below).

Calculation of the Degree of Oxidation. Oxidation of cysteine residues in a zinc finger resulted in the formation of disulfide bonds with the loss of two protons for each disulfide formed. Thus, the degree of peptide oxidation was calculated by determining the amount of oxidized peptide present (M_r lower than that of the reduced peptide by 2*n*, where n = the number of disulfides), compared with the amount of reduced peptide present, based on the heights of the isotopically resolved peaks. The peak height of the reduced form was corrected by subtracting the isotopic contribution of the third isotopic peak of the oxidized form. Because there are no trypsin cleavage sites in zinc finger 1, the entire four-cysteine structure was observed intact, containing none, one, or two disulfide bonds. Therefore, calculation of the amount of singly oxidized peptide (one disulfide bond) was corrected by subtracting the contribution of the third isotopic peak of the doubly oxidized peptide (two disulfide bonds); the peak height of the reduced peptide was corrected for the contribution of the fifth isotope of the doubly oxidized peptide and the third isotope of the singly oxidized peptide. Zinc finger 1 was actually represented by two overlapping peptides corresponding to amino acids 17−47 and 20−42. The results from these two peptides were averaged to give the percent oxidation of zinc finger 1. Baseline levels of oxidation observed in the absence of any added oxidant were subtracted from the data.

For zinc finger 2, there are four possible trypsin cleavage sites (Figure 1). The data from two peptides spanning amino acids 48−67 and 48−69 were averaged to give the percent oxidation of the first half ($ZF2_{C1-2}$). Although two peptides were also observed representing the second half of zinc finger two, i.e., amino acids 71−77 and 72−77, the peak for amino acids 71−77 was usually weak and in a more noisy region of the spectrum. Thus, only the amino acids 72−77 peptide fragment was used in the calculation of the percent oxidation of the second half of finger 2 ($ZF2_{C3-4}$).

Oxidation of methionine to methionine sulfoxide was monitored in the same experiment as a function of oxidant concentration by observing the formation of peaks corresponding to the addition of one oxygen atom, i.e., 16 Da. Methionine residues selected for observation were Met_{56}, immediately adjacent to Cys1 of finger 2, and Met_{86} and Met_{87} situated just after the C-terminal helix of this finger.

Circular Dichroism Spectroscopy (CD). CD spectra were recorded with 10 μM ER-DBD or 25 μM Pep1 or Pep2 in 1 mM DTT, 20 mM sodium phosphate, 100 mM sodium fluoride at pH 7.5, with and without added zinc. Oxidation of ER-DBD by hydrogen peroxide was carried out in 100 mM sodium fluoride/20 mM sodium phosphate, pH 7.4/0.1 mM DTT/60 μM Zn^{2+}, with 0, 1, 2, 3, and 7.5 mM hydrogen peroxide; samples were incubated for 15 min before analysis. The spectropolarimeter (Jasco model 720, Easton, MD) continuously purged with dry nitrogen was scanned over the range 190−260 nm, as previously described (*7*, *26*). Calibration was carried out using an aqueous solution of (+)-10-camphorsulfonic acid. Spectra were accumulated using a 0.1 cm path-length cylindrical quartz cell at room temperature, and buffer spectra obtained under the same conditions were subtracted. The α-helical content was estimated using the Variable Selection method (*27*).

Molecular Graphics. Coordinates for the NMR structure of ER-DBD from Schwabe et al. (*24*) shown in Figure 1B were downloaded from the Protein Data Bank (http://www.rcsb.org) as a PDB file (1HCP). The graphic image was produced using the MidasPlus package from the Computer Graphics Laboratory, UCSF.

RESULTS

Recombinant ER-DBD. The DNA-binding domain of the estrogen receptor (ER-DBD) consisting of approximately 84 residues of a 67 kDa protein was expressed in *E. coli* as a His-tagged protein of 99 amino acids (Figure 1) and purified by IMAC. After confirming that this protein gave a positive EMSA response for binding to the cognate estrogen response element (ERE), its identity and properties were probed by mass spectrometry. Protein eluted from the IMAC column in 8 M urea was dialyzed against 0.1 mM DTT in water, then analyzed by HPLC-MS using ESI-MS. Some samples were subjected to chemical treatments such as oxidation, reduction, or alkylation before separation and analysis by HPLC-MS. Other experiments were conducted by direct infusion of samples into the ESI mass spectrometer without HPLC separation.

Independent measurements were made on various ER-DBD samples. The UV chromatogram and total ion current

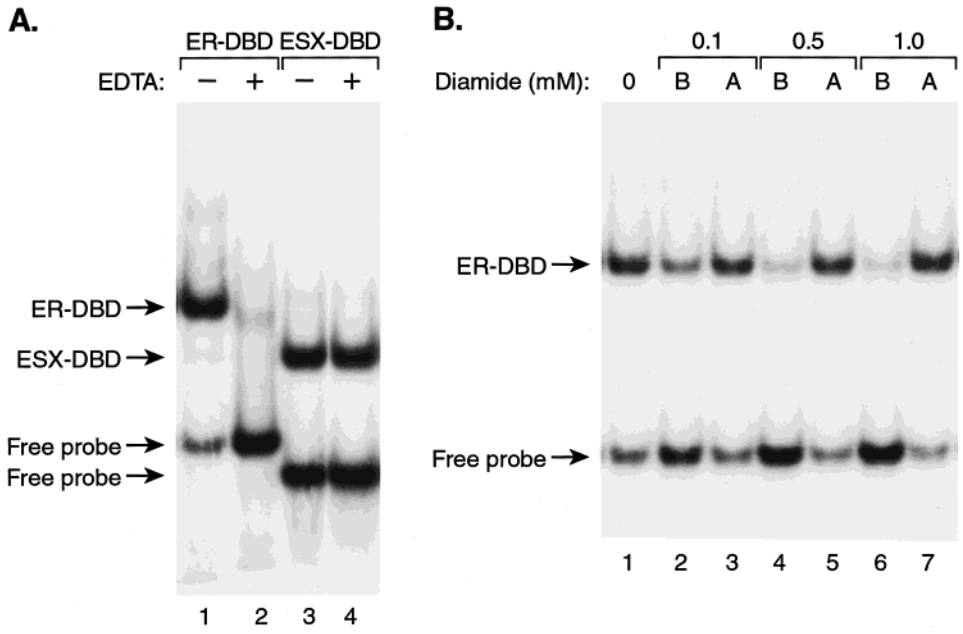

FIGURE 4: Zinc and redox dependent binding of the ER-DBD to an ERE-containing DNA probe. DNA binding by recombinant test (ER-DBD) and control (ESX-DBD) proteins were assessed by EMSA, as described in the Materials and Methods, under either zinc chelation (EDTA) or thiol oxidation (diamide) conditions. (A) EDTA (10 mM) eliminates ER-DBD binding to the ERE-containing DNA probe (lanes 1 and 3), but has no effect on the DNA binding capacity of a control Ets domain (ESX-DBD) that does not bind zinc (lanes 2 and 4). The ESX-DBD probe (containing a cognate Ets response element) is shorter than the ER-DBD probe and the ESX-DBD protein is smaller than the ER-DBD protein, accounting for the faster mobilities of the ESX-DBD complex and free probe. (B) Pretreatment of ER-DBD with 0.1, 0.5, and 1 mM diamide *before* attempted binding to DNA (denoted by B) results in increasing inhibition of DNA binding (lanes 2, 4, and 6). In contrast, treatment with diamide *after* binding ER-DBD to the DNA probe (denoted by A) protects the zinc finger complex from diamide-induced thiol oxidation and loss of its DNA binding capacity (lanes 3, 5, 7).

trace for a typical HPLC separation showed a single chromatographic peak, but ESI-MS revealed that this contained two coeluting components (Figure 2A). Some preparations contained a higher proportion of the second component, but both mass spectrometric peaks were observed in all cases. The measured M_r of the lower mass component (11 232.7 Da) was close to that calculated for ER-DBD (11 232.9 Da), whereas the mass of the second component was higher by ~14 Da. Digestion with trypsin and HPLC-MS separation (not shown) gave a series of peptides. Only the N-terminal peptide Met_1-Lys_{16} was seen as two components, one having the calculated mass and the other being higher by 14 Da. By contrast, a shorter peptide Gly_3-Lys_{16} showed only a single peak of the correct mass. This identified the location of the +14 adduct as either the first or second amino acid in the N-terminal leader sequence (MetLys), probably resulting from methylation of the N-terminal amino group during protein expression. Losses or modifications of N-terminal methionine residues of recombinant proteins have been reported previously (*28*, *29*). The behavior of ER-DBD and component 2 were identical with respect to oxidation, reduction, alkylation, and zinc binding of the zinc fingers, consequently, the inability to separate these species did not affect the aims of this study.

After reduction with DTT, ER-DBD was treated with iodoacetic acid (IAA) to carboxymethylate the thiol groups, each of which should increase the molecular mass by 58 Da. A mixture of products was obtained, the most abundant of which corresponded to the alkylation of eight or nine of the nine cysteines (Figure 2B). A minor degree of overreaction gave other weaker peaks for the addition of 10 and 11 carboxymethyl groups. As anticipated, ER-DBD that had been oxidized with hydrogen peroxide then treated with IAA proved to be resistant to carboxymethylation (not shown). Thus we confirmed that ER-DBD reduced with DTT had the anticipated number of free thiols.

Monitoring oxidation of ER-DBD by HPLC-MS. ER-DBD contains nine cysteines and five methionines. Treatment of ER-DBD with hydrogen peroxide induced two different types of oxidation, (i) the loss of one or more pairs of hydrogen atoms as disulfide bonds were formed, and (ii) the addition of multiple oxygen atoms, almost certainly to form methionine sulfoxide (Figure 3). Peroxide treatment at 5 mM for 25 min removed only four hydrogens and added zero, one or two oxygens (Figure 3A), whereas overnight treatment removed six hydrogens and added one to five oxygens (Figure 3B). After oxidation for 25 min, further treatment with 50 mM DTT reduced the disulfide bonds but did not reduce the methionine sulfoxides (Figure 3C). Diamide [$(CH_3)_2N{\cdot}CO{\cdot}N{=}N{\cdot}CO{\cdot}N(CH_3)_2$] is a reagent that specifically oxidizes cysteine to cystine (*30*). Treatment with 5 mM diamide for 25 min partially oxidized ER-DBD by the removal of an average of four hydrogen atoms (Figure 3D), whereas 25 mM diamide removed eight hydrogens but also gave rise to a new species corresponding to the addition of a diamide molecule (Figure 3E). Treatment with DTT reduced the cystines back to cysteine and removed the diamide adduct (Figure 3F). Unlike peroxide, diamide induced very little methionine sulfoxide formation.

DNA-Binding Is Zinc Dependent and Protects ER-DBD against Oxidation. As was demonstrated previously (*17*), EMSA shows that EDTA destroys the ability of ER-DBD to bind to an ERE-containing DNA probe (Figure 4A, lanes 1 and 3) unlike a control DBD (ESX) that binds monomerically to DNA but does not contain a zinc finger (lanes 2 and 4). This is fully consistent with the known role of the

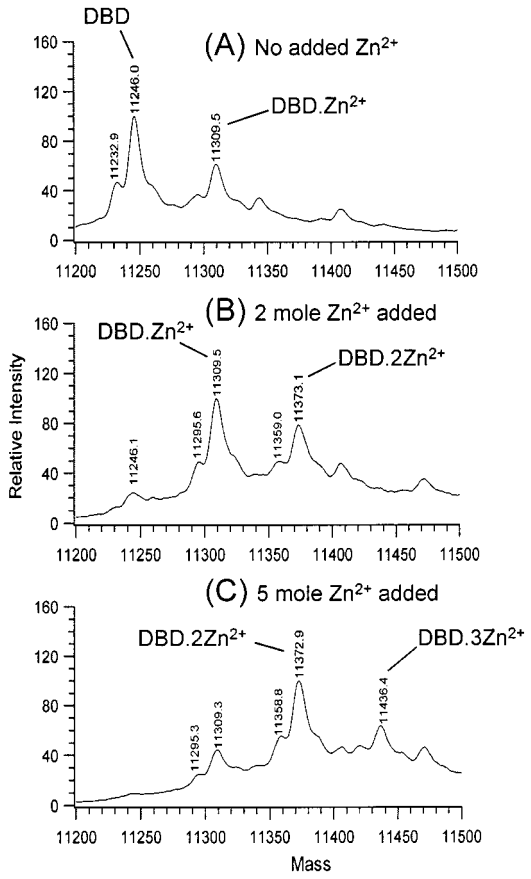

FIGURE 5: Deconvoluted mass spectra showing Zn^{2+} binding to ER-DBD at pH 7.4 monitored by ESI-MS. Data averaged from several measurements showed a mass increase of 63.5 Da for each zinc ion added, due to elimination of two protons per Zn^{2+}. (A) ER-DBD purified from the expression system without added zinc. The major peak at 11246.0 Da (DBD) is the methylated species and the weaker peak at 11309.9 Da is DBD plus one zinc ion. The species 11343.7 and 11408.2 Da are probably due to the addition of sulfate from $CaSO_4$. (B) ER-DBD in a buffer containing 2 mol of zinc per mole of protein. The free DBD peak (11246.1 Da) is minor compared with the complexes containing one (11309.5 Da) or two (11373.1 Da) zinc ions. (C) ER-DBD in a buffer containing 5 mol of zinc/mol of protein. The major species is the addition of 2 zinc ions, with weaker addition of a third zinc ion (11436.4 Da), perhaps to the His tag.

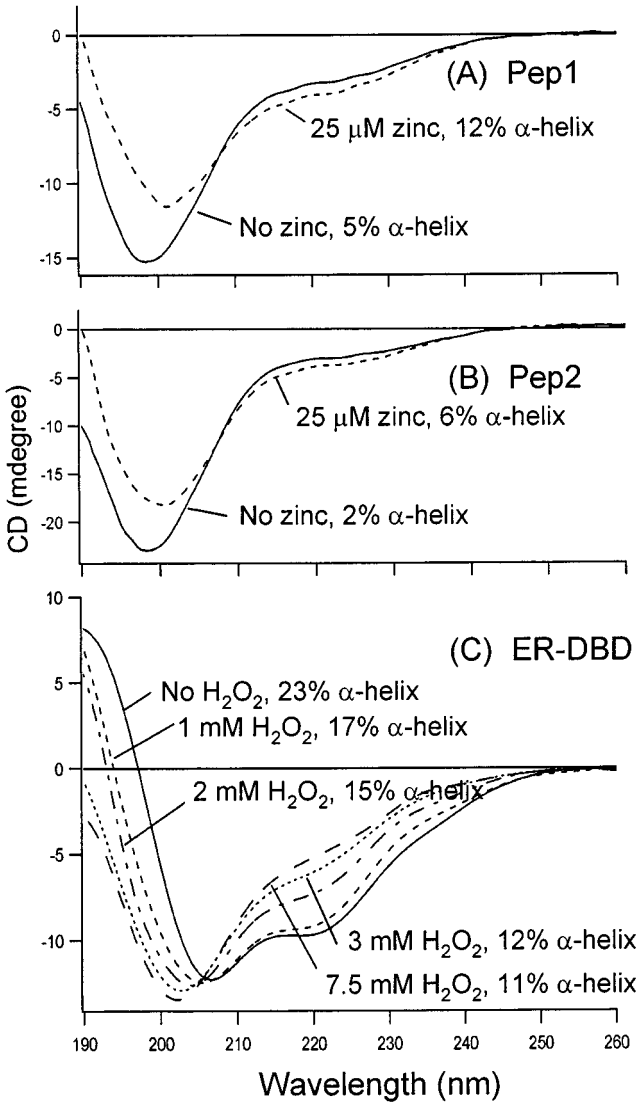

FIGURE 6: (A) CD spectra of 25 μM Pep1 in 100 mM sodium fluoride/20 mM sodium phosphate, pH 7.4/1 mM DTT, with 0 and 25 μM Zn^{2+}. (B) CD spectra of Pep2 as above. (C) 10 μM ER-DBD in 100 mM sodium fluoride/20 mM sodium phosphate, pH 7.4/0.1 mM DTT/60 μM Zn^{2+}, with 0, 1, 2, 3, and 7.5 mM hydrogen peroxide. In every case, the α-helix content was estimated using the Variable Selection method (*27*).

zinc fingers in stabilizing the structure of ER-DBD. For ER-DBD treated with oxidant before (B) exposure to the ERE-containing DNA probe, even 0.1 mM diamide was sufficient to significantly reduce the level of DNA binding achieved and higher concentrations completely destroyed binding (Figure 4B, lanes 1, 3, and 5). By contrast, when the treatment with oxidant was after (A) exposure to the DNA probe, even 1 mM diamide was unable to inhibit DNA binding (lanes 2, 4, and 6).

Stoichiometry of Zinc Binding to ER-DBD Monitored by ESI-MS. Recombinant ER-DBD that had not been purified by HPLC was monitored by ESI-MS in a weak buffer at pH 7.4, conditions that should allow observation of intact noncovalent complexes and reveal the stoichiometry of any complex formed between the protein and zinc ions. The strongest peak (M_r 11 246.0 Da, methylated species) representing approximately two-thirds of the protein was free of zinc, whereas one-third of the protein showed the addition of a single Zn^{2+} cation (mass 11 309.5 Da) (Figure 5A). There was no observable addition of two Zn^{2+} ions. No zinc had been added at any stage in the expression or purification; therefore, it was concluded that the protein had scavenged the zinc from the cells in which it was expressed. The presence of less than the stoichiometric amount of zinc was consistent with a CD spectrum showing a lower than normal degree of α-helicity compared with fully zinc-loaded ER-DBD, which shifted to higher helix content upon addition of zinc (not shown).

ESI-MS was also used to monitor further addition of Zn^{2+}. Titration of the protein with 2 mol of the metal cation/mol of reduced ER-DBD showed strong formation of the complex ER-DBD.Zn^{2+} and a lesser amount of ER-DBD·2Zn^{2+} (mass 11 373.1 Da) (Figure 5B). The CD spectrum confirmed that this amount of zinc was sufficient to restore the α-helicity to its normal level (Figure 6C). Exposure of ER-DBD to 5 mol of zinc/mol of protein caused the ER-DBD·2Zn^{2+} peak to become the most intense in the mass spectrum. Weak binding of a third zinc ion was also seen to occur (mass 11 436.4 Da), possibly by binding to the His tag or simply

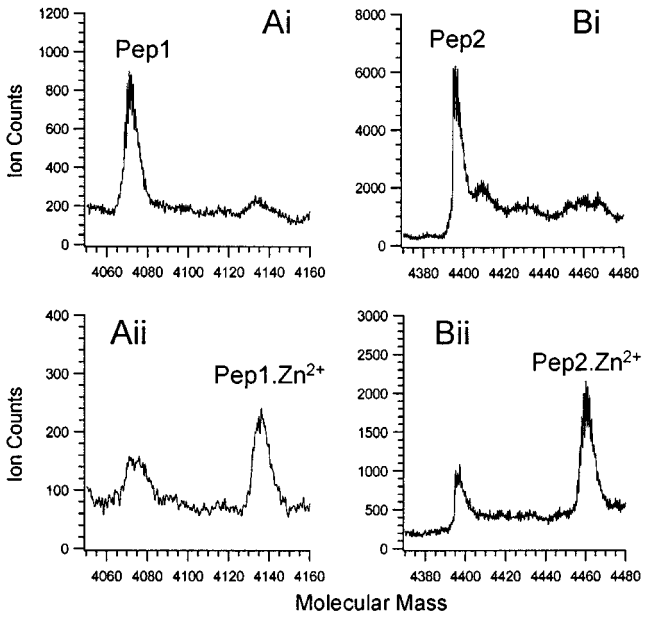

FIGURE 7: Deconvoluted ESI mass spectra showing Zn^{2+} binding to the synthetic peptides Pep1 and Pep2 at pH 7.4. (A) 10 μM Pep1 (i) without added zinc, (ii) with 10 μM zinc. (B) Pep2 as above. In both cases, the spectra show the binding of a single zinc ion by ~70% of the peptide molecules.

as a nonspecific effect of ESI-MS. After oxidation with either peroxide or diamide, ESI-MS confirmed that ER-DBD could bind only low levels of zinc in a nonspecific manner (not shown), again, perhaps involving the His tag. This observation was consistent with our previous finding that oxidation of ER-DBD destroyed α-helix and prevented DNA binding (*7*).

The precision of the ESI-MS mass measurements for ER-DBD·$2Zn^{2+}$ was sufficient to establish that the binding of two zinc ions involved the elimination of four protons from ER-DBD, i.e., on average each zinc ion added only 63.5 Da to the mass, even though the average atomic mass of zinc is 65.5 Da. Four cysteine residues participate in stabilizing each of the two zinc fingers, thus it can be concluded that each finger involves two thiolate anions forming ionic bonds and two thiols forming coordinate bonds. A similar observation by ESI-MS was also reported for a Cys_3His zinc finger (*31*).

Action of the Two Zinc Fingers in Stabilizing the Structure Is Cooperative. It was reported that upon addition of Zn^{2+}, the second zinc finger from the glucocorticoid receptor (GR) synthesized as an isolated peptide could form an α-helix and bind to DNA (*32*). This DNA binding was somewhat unexpected as hormone receptors such as ER and GR bind to DNA as dimers and the X-ray structure of the ER-DBD/ERE/Zn^{2+} complex shows cooperativity between the two fingers, the first binding to the recognition element and the second stabilizing the ER-DBD dimer (Figure 1B). To compare the ER fingers with the reported behavior of GR, both were synthesized as separate peptides, Pep1 and Pep2 (Figure 1) and probed by EMSA, ESI-MS, and CD. There was no evidence from EMSA that either peptide was able to bind to ERE (not shown). Nevertheless, zinc titrations by ESI-MS showed that, with a peptide:Zn^{2+} molar ratio of 1:1, each peptide strongly bound a single Zn^{2+} ion (Figure 7). At higher Zn^{2+} concentrations (not shown), Pep1 showed very little sign of binding further zinc, but became less soluble and tended to precipitate. By contrast, Pep2 remained soluble and was able to bind a second Zn^{2+} ion, although with lower affinity.

The effect of Zn^{2+} on the secondary structures of these peptides was monitored by CD spectroscopy and compared with the behavior of ER-DBD (Figure 6). We had previously established that salt at near-physiological concentration was necessary for ER-DBD to maintain its structure (*7*); therefore, the same was assumed to be true of the individual peptides. Buffers containing 100 mM sodium fluoride were used for all CD experiments, rather than sodium chloride as the chloride ion absorbs UV radiation below 200 nm. The CD spectrum of a typical random coil structure should show a minimum at ~195 nm and relatively little signal at ~222 nm, whereas α-helical proteins generally show a maximum at ~195 nm and two minima at 208 and 222 nm that correspond to $\pi-\pi^*$ and $n-\pi^*$ electronic transitions, respectively. As seen in Figure 6, panels A and B, in the absence of zinc, both synthetic peptides showed minima strongly blue-shifted from the α-helix value to ~198 nm and very weak signals at 222 nm. This was indicative of low α-helix content, which was confirmed by secondary structural analysis, giving only 5% α-helix for Pep1 and 2% for Pep2. Furthermore, there were only weak increases in α-helical structure on the addition of 1 M equiv of Zn^{2+}, particularly for Pep2 for which the α-helix increased to only 6%, despite the relatively strong zinc-binding properties of both peptides demonstrated by ESI-MS. There were no further increases in α-helicity on addition of higher concentrations of zinc (not shown), but for Pep1, there was a loss of signal as the peptide precipitated. For neither peptide was the α-helical content comparable to that of ER-DBD itself. The CD spectrum of ER-DBD obtained in the presence of excess zinc (Figure 6C, solid line), with strong minima at 207 and 222 nm and a maximum at 190 nm, gave an estimated α-helix content of ~23%. This spectrum is similar to one we reported earlier for a different preparation of ER-DBD, from which we calculated 28% α-helix (*7*).

The failure of Pep2 to form significant α-helix in the presence of zinc is in contrast to the reported behavior of an analogous peptide for GR. However, this observation is consistent with recent NMR studies that have shown that the helical structure of finger 2 in GR-DBD is more stable than that of ER-DBD (33).

Differential Susceptibility of the Two Fingers in ER-DBD to Thiol Oxidation. The sensitivity of ER-DBD/DNA binding to thiol oxidation has been established previously (*7*). Initial experiments on the oxidation of ER-DBD described above showed that limited oxidation could be achieved in which only four out of a possible eight hydrogens were eliminated from the fully reduced protein (Figure 3), but it was not known whether this was due to selective oxidation of a single finger or a random effect on both fingers. To probe this further, conditions were sought that would allow a comparison of the susceptibilities of zinc fingers 1 and 2 to oxidant stress under different conditions. ER-DBD was oxidized with increasing concentrations of either hydrogen peroxide or diamide in the presence of zinc, rapidly proteolyzed using an immobilized trypsin column, then the resulting peptides were eluted directly onto a high throughput HPLC column for HPLC-MS analysis. ER-DBD has an unequal distribution

of basic residues (trypsin and arginine), none of which is in finger 1; therefore, this would not be cleaved by trypsin but should create a single 23-residue peptide $Tyr_{20}-Lys_{42}$ containing all four cysteines ($ZF1_{Cys1-4}$). Zinc finger 2 has four basic residues between Cys2 and Cys3 and should be cleaved to give two major peptides of twenty amino acids $Ser_{48}-Lys_{67}$ containing the first two cysteines ($ZF2_{Cys1-2}$), and six amino acids $Ser_{72}-Arg_{77}$ containing the second two ($ZF2_{Cys3-4}$). It was anticipated that the molecular masses of individual peptides would reveal whether the cysteines in each peptide were reduced or oxidized. Furthermore, disulfide cross-linking between $Ser_{48}-Lys_{67}$ and $Ser_{72}-Arg_{77}$ would be a potential product of oxidation in finger 2.

Initially, the resulting peptides were found to be prone to oxidation during digestion and chromatography, probably due to dissolved air, even though the digestion time was limited to 3 min. To minimize unwanted oxidation, dissolved air was removed from all solutions by vacuum filtration immediately prior to their use and maintenance of all solutions under a positive pressure of helium. Partial oxidation of peptides from zinc finger 2, each containing two cysteines, would give two species differing in mass by 2, whereas those from finger 1 containing four cysteines could give peaks for species that were reduced, partly oxidized (−2) and fully oxidized (−4). This analysis was made more complicated by overlap of isotope patterns and the fact that the ions in ESI-MS had multiple charges, usually 2 or 3. Additional peptides coming from incomplete digestion were identified, such as 70−77 with a proportion of the N-terminal lysine not being removed by trypsin.

The target peptides were identified from an analysis of the multiply charged ions in the HPLC-MS spectra (e.g., Figure 8A), from which the relative abundances of the reduced and oxidized forms were calculated. Taking account of the isotope corrections, the amount of oxidation occurring under different conditions was calculated for different concentrations of oxidant. This revealed only low levels of oxidation of finger 1 under conditions that caused extensive oxidation of finger 2; furthermore, the oxidation of finger 2 was asymmetric, with a much higher level of disulfide formation between cysteines 3 and 4 than between 1 and 2. This is illustrated in Figure 8B for oxidation by hydrogen peroxide, showing that 2 mM peroxide was sufficient to oxidize 100% of $ZF2_{Cys3-4}$ whereas 7.5 mM was not sufficient to fully oxidize any of the other pairs of cysteines. Similar trends were observed with 0−500 μM diamide in the presence of zinc ions, as is summarized for 300 μM diamide in Figure 8C. Interestingly, the removal of zinc by EDTA increased the sensitivity of finger 1 to oxidation such that both fingers were oxidized to the same degree (Figure 8C). The observation that finger 1 is more resistant to oxidation than finger 2 only when zinc ions are present and not in the absence of zinc strongly supports structural studies by NMR that zinc in finger 2 is less well coordinated than in finger 1 (*33*).

If the tetrahedral arrangement of the cysteine residues was maintained during oxidation, within a single finger there would be equal cross-linking of peptides by disulfide formation between Cys1−Cys2/Cys3−Cys4, Cys1−Cys3/Cys2−Cys4, and Cys1−Cys4/Cys2−Cys3. Statistically, a tryptic digest of finger 2 should reveal twice the abundance of the cross-linked peptides such as 48−67/72−77 compared with the separate oxidized peptides 48−67 and 72−77. However, the signal for the cross-linked peptide was of much lower intensity (~10%) than the separate peptides, suggesting that oxidation disrupts the geometry and expels the Zn^{2+} ion from this finger before the disulfide bonds are formed. It was not possible to make a direct comparison with the behavior of finger 1 as this was not cleaved by trypsin, but HPLC separation of the fully oxidized species gave three peaks of approximately equal abundance, which are likely attributable to the three different disulfide-bonded isomers.

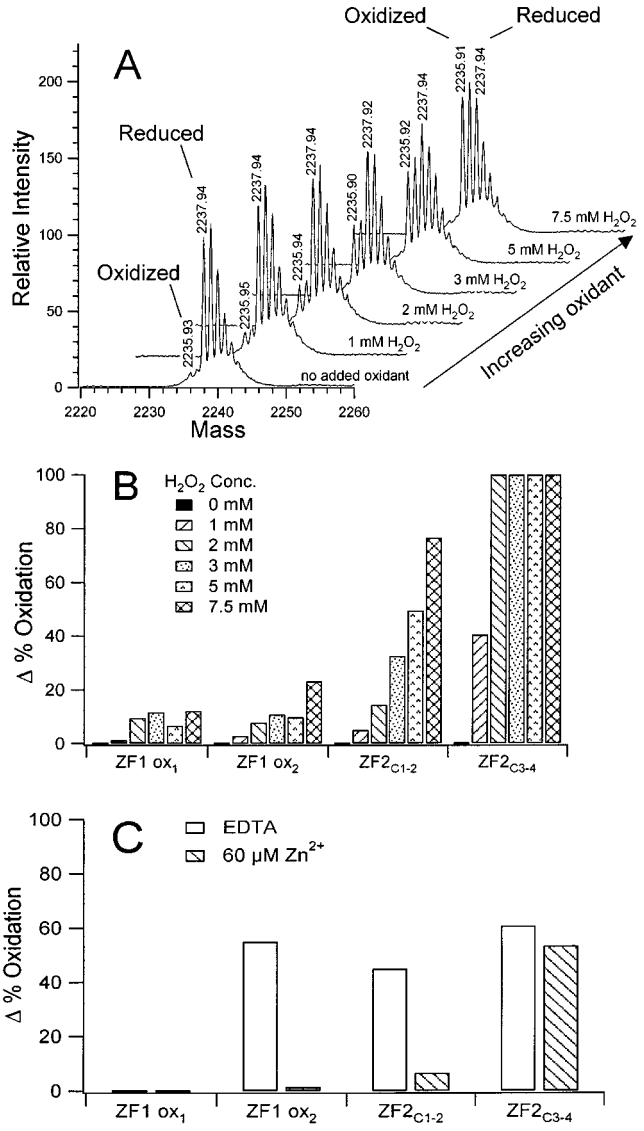

FIGURE 8: (A) Deconvoluted molecular ion profile of peptide $Ser_{48}-Lys_{67}$ ($ZF2_{C1-2}$) of M_r 2237.9 Da, after oxidation of zinc-loaded ER-DBD by H_2O_2, digestion with trypsin then rapid HPLC-MS. This shows increasing abundance of oxidized peptide (M_r 2235.9 Da, i.e., two Hs less) with one disulfide bond. (B) Histograms showing the relative increase in oxidation of the various tryptic peptides with increasing H_2O_2 concentration in the presence of zinc. All four cysteines of zinc finger 1 are contained within a single peptide, seen as singly oxidized (ox_1, −2 H), or doubly oxidized (ox_2, −4 H). The four cysteines of zinc finger 2 are separated into the two peptides $ZF2_{C1-2}$ and $ZF2_{C3-4}$, each of which can be oxidized with loss of 2H. (C) Similar oxidation of ER-DBD by 300 μM diamide, after removal of zinc ions by EDTA (open bars) and with 60 μM zinc (cross-hatched bars).

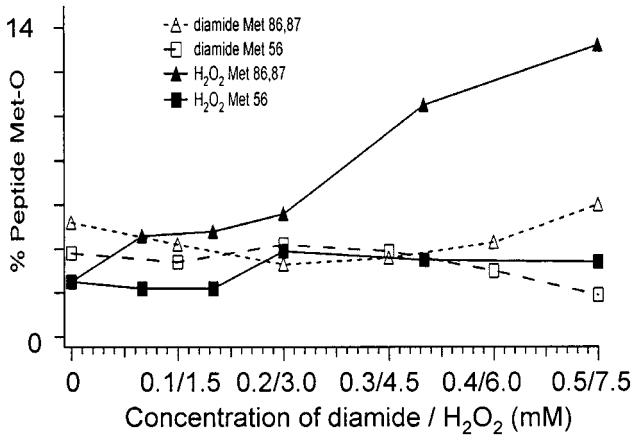

FIGURE 9: Oxidation of methionine to methionine sulfoxide by diamide (open symbols) or H_2O_2 (solid symbols) as monitored by a mass increase of 16 Da for peptides containing Met_{56} (squares) or both Met_{86} and Met_{87} (triangles).

This would indicate that the finger structure was maintained more strongly during oxidation of finger 1 than 2.

Oxidation of ER-DBD by Hydrogen Peroxide Monitored by CD. Having established by ESI-MS that 15 min exposure to as little as 2 mM hydrogen peroxide strongly disrupts and oxidizes zinc finger 2 and that 7.5 mM causes significant oxidation to finger 1, the effect of increasing peroxide concentration over this range was monitored by CD. The CD curves in Figure 6C demonstrate a progressive blue-shift of the $\pi-\pi^*$ minimum from 207 to 202 nm and a steady reduction in the $n-\pi^*$ signal at 222 nm, with a corresponding diminution of the α-helix content from 23 to 11%. There was no further change in the spectrum upon further addition of peroxide (not shown), indicating that the zinc finger structure of ER-DBD was completely disrupted by 7.5% peroxide. Interestingly, this suggests that the remaining 11% α-helix is independent of the zinc-containing motifs.

Methionine Oxidation Does Not Protect against Thiol Oxidation. It has been proposed that methionine residues at strategic sites in proteins might act as scavengers for oxidative species and thereby protect cysteine thiols from oxidation (*34*). We had already established that 5 mM peroxide could partially oxidize both methionine and cysteine in ER-DBD (Figure 3). Additional data from the titrations described above (Figure 8) allowed a comparison between the levels of oxidant required to achieve a high level of thiol oxidation at any site and the amount of methionine sulfoxide formed by selected methionine residues. For example, peptide $Ser_{48}-Lys_{67}$ contains a single methionine (Met_{56}) immediately adjacent to $ZF2_{Cys1}$; although a background level of ~3−4% oxidation was observed for this methionine, this did not increase at all upon exposure to up to 7.5 mM hydrogen peroxide or 500 mM diamide, even though these amounts were sufficient to completely disrupt and oxidize finger 2 (Figure 9). Furthermore, two other methionine residues (Met_{86} and Met_{87}) situated just outside the C-terminus of the finger 2 helix, showed very limited oxidation totaling less than 10% above baseline upon exposure to up to 7.5 mM peroxide and no significant oxidation upon exposure to diamide. Thus, contrary to the suggestion that methionine might protect against oxidation (*34*), the zinc finger cysteines are more susceptible to oxidation than any of the three methionine residues contained in the ER-DBD.

Scheme 1: Unstructured Monomeric ER-DBD Binds Two Zn^{++} Ions that Induce Structure in Both the DNA-Binding and Dimerization Motifs[a]

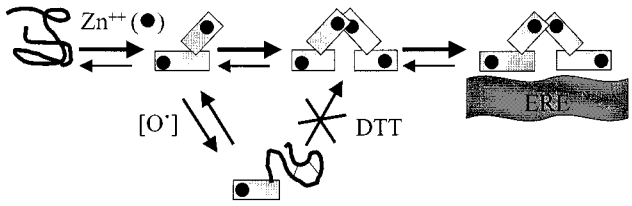

[a] It can then dimerize to bind to an ERE-containing DNA. Oxidation of the less structured dimerization motif supported by ZF2 expels the zinc ion with formation of disulfide bonds that prevent dimerization and DNA binding.

DISCUSSION AND CONCLUSIONS

Although X-ray crystallography established that the dual zinc finger motif of ER-DBD plays a central role in binding protein dimers to DNA (*23*), NMR has shown that the structure of free monomeric ER-DBD in solution is little different from that of the DNA bound protein (*23*, *33*). We have previously demonstrated that thiol-reactive oxidants disrupt the DNA-binding properties and the α-helical structure of ER-DBD in a reversible manner, whereas cysteine alkylation permanently destroys these characteristics (*7*). In the present work, we have extended these studies to demonstrate that oxidation has an asymmetric effect, leading to elimination of zinc ions from zinc loaded ER-DBD, with finger 2 being much more sensitive to the action of agents such as hydrogen peroxide and diamide than finger 1.

The EMSA results shown here demonstrate that ER-DBD bound to DNA is protected from oxidation relative to ER-DBD free in solution. In the biological situation the turnover of protein ensures that at any given time, a proportion of ER-DBD is not complexed. Consequently, the sensitivity to oxidation of the monomeric form in solution is directly relevant to the potential impairment of DNA binding caused by oxidation. Although the functions of the two zinc fingers of ER-DBD can be viewed separately in that the first participates directly in DNA binding, whereas the second is involved in dimerization, they are cooperative in maintaining secondary and tertiary structure with dimerization being essential to stabilize DNA binding. Thus, damage to either zinc finger could have a critical impact on the normal transcriptional role of ER. It should be noted that the ER-LBD contains a distinct dimerization motif (*35*), which is dependent upon both ligand and DNA binding, but this alone is unable to compensate for the loss of the second zinc finger function. Data presented here strongly implicate the more loosely structured ER-DBD zinc finger 2 as the most likely site for oxidative and structural damage associated with loss of intracellular ER function.

The proposed ER susceptibility to oxidative damage is illustrated in Scheme 1. In the absence of zinc ions, ER-DBD is monomeric and largely unstructured, but it has a high affinity for zinc and readily binds two Zn^{2+} ions that induce α-helical structure in both the DNA-binding motif and the dimerization motif (represented as rectangles), allowing pairs of ER-DBD molecules to dimerize and bind to an ERE-containing DNA with nanomolar affinity (*17*). In solution, however, even after binding zinc, the more

loosely structured dimerization motif supported by zinc finger 2 is susceptible to oxidation. This expels the zinc ion with formation of disulfide bonds, giving a form of the molecule that can no longer dimerize or stably bind DNA. While this thiol oxidative process is reversible in vitro, a reducing environment is necessary for this reversal; tissues subjected to aging or hypoxia-reperfusion (e.g., tumors outgrowing their vascular supply) may be unable to sustain such a reducing environment. The well-described phenomenon of hypoxia-reperfusion injury is widely recognized as the inducer of myocardial, brain and other organ damage from vascular disease. Here significant free radical formation and cellular injury occur not during the hypoxia phase (which constitutes a reducing environment), but rather during the subsequent reperfusion phase. The reperfusion phase brings oxygenated blood/nutrients that produce local membrane and intracellular increase in nitric oxide and lipid peroxidation products, resulting in cellular and subcellular oxidative damage. We (*7*) and others (*36*) have suggested that this also happens on a regular basis with solid tumors growing in vivo as the expanding tumor edge outstrips its vascular supply and later gets refed with new vessel growth or as a result of regular variations in red blood cell flux through the tumor microvasclature; in particular, Kimura et al. have documented this phenomenon of transient hypoxia and reoxygenation within tumor parenchyma (*36*). Thus, as noted previously (*7*), it is reasonable to suggest that human breast tumors subjected to repeated oxidative stress may express transcription factors with altered DNA-binding and gene regulating activities, determining a more aggressive clinical phenotype. The sustained production of free radicals and reactive oxygen species may also lead to irreversible alkylation with permanent loss of ER DNA-binding function.

It may also be relevant to consider the potential functional impact of DNA-binding-impaired ER in view of surprising in vivo results observed with DNA-binding-impaired GR. Although transcriptional regulation by GR is essential for survival, it has been shown that genetically engineered complete loss of DNA-binding function has less than lethal organismal and cellular consequences (*37*), contrary to the previously accepted view that GR DNA binding was absolutely essential for viability (*38*, *39*). This conclusion was demonstrated by insertion of a point mutation Ala458Thr in the GR gene of transgenic mice that resulted in a dimerization-defective receptor that no longer bound to the palindromic GR DNA response element. In contrast to GR null (−/−) mice, these DNA-binding-impaired mutant mice proved to be viable and developed as relatively normal, healthy animals, thereby revealing the importance of DNA-binding-independent GR function, presumably due to direct protein−protein gene regulating GR mechanisms. In light of these GR results, the functional consequences of oxidant-induced loss of ER DNA binding remain to be explored in much greater depth.

ACKNOWLEDGMENT

R.M.W. thanks the Natural Sciences and Engineering Research Council of Canada for a postdoctoral fellowship. We thank Dr. Shauna Farr-Jones for assistance with molecular graphics.

REFERENCES

1. Sun, Y., and Oberley, L. W. (1996) *Free Radical Biol. Med. 21*, 335−348.
2. Wu, X., Bishopric, N. H., Discher, D. J., Murphy, B. J., and Webster, K. A. (1996) *Mol. Cell. Biol. 16*, 1035−1046.
3. Hayashi, S.-I., Harjiro-Nakanishi, K., Makino, Y., Eguchi, H., Yodoi, J., and Tanaka, H. (1997) *Nucleic Acids Res. 25*, 4035−4040.
4. Klug, A., and Schwabe, J. W. R. (1995) *FASEB J. 9*, 597−604.
5. Suske, G. (1999) *Gene 238*, 291−300.
6. Cano-Gauci, D. F., and Sarkar, B. (1996) *FEBS Lett. 386*, 1−4.
7. Liang, X., Lu, B., Scott, G. K., Chang, C.-H., Baldwin, M. A., and Benz, C. C. (1998) *Mol. Cell Endocrinol. 146*, 151−161.
8. Scott, G. K., Kushner, P., Vigne, J. L., and Benz, C. C. (1991) *J. Clin. Invest. 88*, 700−706.
9. Montgomery, P. A., Scott, G. K., Luce, M. C., Kaufmann, M., and Benz, C. C. (1993) *Breast Cancer Res. Treat. 26*, 181−189.
10. Johnston, S. R. D., Lu, B., Dowsett, M., Liang, X., Kaufmann, M., Scott, G. K., Osborne, C. K., and Benz, C. C. (1997) *Cancer Res. 57*, 3723−3727.
11. Witkowska, H. E., Carlquist, M., Engstrom, O., Carlsson, B., Bonn, T., Gustaffson, J.-Å., and Shackleton, C. H. L. (1997) *Steroids 62*, 621−631.
12. Seielstad, D. A., Carlson, K. E., Kushner, P. J., Greene, G. L., and Katzenellenbogen, J. A. (1995) *Biochemistry 34*, 12605−12615.
13. Fenn, J. B., Mann, M., Meng, C. K., Wong, S. K., and Whitehouse, C. M. (1990) *Mass Spectrom. Rev. 9*, 37-.
14. Loo, J. A. (1997) *Mass Spectrom. Rev. 16*, 1−23.
15. Last, A. M., and Robinson, C., V. (1999) *Curr. Opin. Chem. Biol. 3*, 564−570.
16. Witkowska, H. E., Green, B. M., Carlquist, M., and Shackleton, C. H. (1996) *Steroids 61*, 433−438.
17. Predki, P. F., and Sarkar, B. (1992) *J. Biol. Chem. 267*, 5842−5846.
18. Hutchens, T. W., and Allen, M. H. (1992) *Rapid Commun. Mass Spectrom. 6*, 469−473.
19. Hutchens, T. W., Allen, M. H., Li, C. M., and Yip, T.-Y. (1992) *FEBS Lett. 309*, 170−174.
20. Witkowska, H. E., Shackleton, C. H. L., Dahlman-Wright, K., Kim, J. Y., and Gustaffson, J.-Å. (1995) *J. Am. Chem. Soc. 117*, 3320−3324.
21. Veenstra, T. D., Benson, L. M., Craig, T. A., Tomlinson, A. J., Kumar, R., and Naylor, S. (1998) *Nat. Biotechnol. 16*, 262−266.
22. Schwabe, J. W. R., Neuhaus, D., and Rhodes, D. (1990) *Nature 348*, 458−461.
23. Schwabe, J. W. R., Chapman, L., Finch, J. T., and Rhodes, D. (1993) *Cell 75*, 567−578.
24. Schwabe, J. W. R., Chapman, L., Finch, J. T., Rhodes, D., and Neuhaus, D. (1993b) *Structure 1*, 187−204.
25. Studier, F. W., Rosenberg, A. H., Dunn, J. J., and Dubendorff, J. W. (1990) *Methods Enzymol. 185*, 60−89.
26. Lu, B., Liang, X., Scott, G. K., Chang, C.-H., Baldwin, M. A., and Benz, C. C. (1998) *Breast Cancer Res. Treat. 48*, 243−257.
27. Johnson, W. C., Jr. (1990) *Proteins 7*, 205−214.
28. Seeger, A., and Rinas, U. (1996) *J. Chromatogr. A 746*, 17−24.
29. Yan, Z., Caldwell, G. W., McDonell, P. A., Jones, W. J., August, A., and Masucci, J. A. (1999) *Biochem. Biophys. Res. Commun. 259*, 271−282.
30. Kosower, N. S., Kosower, E. M., Wertheim, B., and Correa, W. S. (1969) *Biochem. Biophys. Res. Commun. 37*, 593−596.
31. Fabris, D., Zaia, J., Hathout, Y., Fenselau, C., (1996) *J. Am. Chem. Soc. 118*, 12242−12243.
32. Archer, T. K., Hager, G. L., and Omichinski, J. G. (1990) *Proc. Natl. Acad. Sci. U.S.A. 87*, 7560−7564.

33. Wikström, A., Berglund, H., Hambraeus, C., van den Berg, S., and Härd, T. (1999) *J. Mol. Biol. 289*, 963−979.
34. Levine, R. L., Mosoni, L., Berlett, B. S., and Stadtman, E. R. (1996) *Proc. Natl. Acad. Sci. U.S.A.* 93, 15036−15040.
35. Kumar, V., and Chambon, P. (1988) *Cell 55*, 145−156.
36. Kimura, H., Braun, R. D., Ong, E. T., Hsu, R., Secomb, T. W., Papahadjopoulos, D., Hong, K., and Dewhirst, M. W. (1996) *Cancer Res. 56*, 5522−5528.
37. Reichardt, H. M., Kaestner, K. H. Tuckermann, J., Kretz, O., Wessely, O., Bock, R., Gass, P., Schmid, W., Herrlich, P., Angel, P., and Schütz, G., (1998) *Cell 93*, 531−541.
38. Beato, M., Herrlich, P., and Schütz, G. (1995) *Cell 83*, 851−857.
39. Karin, M. (1998) *Cell 93*, 487−490.

BI000282F